SEFRON: A New Spiking Neuron Model With Time-Varying Synaptic Efficacy Function for Pattern Classification

Abeegithan Jeyasothy, Suresh Sundaram, *Senior Member, IEEE*, and Narasimhan Sundararajan, *Life Fellow, IEEE*

***Abstract*—This paper presents a new time-varying long-term Synaptic Efficacy Function-based leaky-integrate-and-fire neuRON model, referred to as SEFRON and its supervised learning rule for pattern classification problems. The time-varying synaptic efficacy function is represented by a sum of amplitude modulated Gaussian distribution functions located at different times. For a given pattern, the SEFRON's learning rule determines the changes in the amplitudes of weights at selected presynaptic spike times by minimizing a new error function reflecting the differences between the desired and actual postsynaptic firing times. Similar to the gamma-aminobutyric acid-switch phenomenon observed in a biological neuron that switches between excitatory and inhibitory postsynaptic potentials based on the physiological needs, the time-varying synapse model proposed in this paper allows the synaptic efficacy (weight) to switch signs in a continuous manner. The computational power and the functioning of SEFRON are first illustrated using a binary pattern classification problem. The detailed performance comparisons of a single SEFRON classifier with other spiking neural networks (SNNs) are also presented using four benchmark data sets from the UCI machine learning repository. The results clearly indicate that a single SEFRON provides a similar generalization performance compared to other SNNs with multiple layers and multiple neurons.**

***Index Terms*—Gamma-aminobutyric acid (GABA)-switch, Synaptic Efficacy Function-based leaky-integrate-and-fire neuRON (SEFRON), spiking neurons, spike-timing-dependent plasticity (STDP), time-varying synaptic efficacy function.**

I. INTRODUCTION

IN RECENT times, spiking neural networks (SNNs) are being developed with increasing interest because of their biologically relevant functionalities and also the high computational power that they possess compared with sigmoidal neural networks. SNNs require a lower number of neurons compared with a sigmoidal neural network for approximating the same function, implying that an SNN is computationally more powerful than a sigmoidal neural network of the same size [1]. From the machine learning point of view, the core research activities in SNNs have been in the areas of developing efficient supervised learning algorithms, such as SpikeProp [2], synaptic weight association training (SWAT) [3], ReSuMe [4], Tempotron [5], and others [6]–[13]. The main objectives of these algorithms have been learning the functional relationships between the input and output spike patterns. Learning algorithms in SNNs employ different neuron models, such as Hodgkin–Huxley model [14], leaky-integrate-and-fire (LIF) model [15], [16], or spike response model (SRM) [17], [18]. In the literature, the most commonly used spiking neuron model for the development of SNNs is the LIF model or its equivalent SRM because of their simpler forms and ease of developing learning algorithms. The SRM uses a kernel integration scheme to determine the postsynaptic potential. An LIF neuron model can be mapped into an SRM where the excitatory and inhibitory postsynaptic potentials (IPSPs) are defined as products of spike response functions and synaptic efficacies [19].

These neuron models provide the flexibility to access the synaptic efficacy directly and develop learning algorithms to adjust it without affecting other neuron properties. In SNNs, two spiking neurons are connected via a synapse model. A synapse model represents the strength of a connection between two spiking neurons. The strength of the connection between the ith input neuron and the jth output neuron is characterized by its weight w_{ij}. This weight determines the amplitude of the postsynaptic response (typically indicated by the height of the postsynaptic potential or the slope of the postsynaptic current). The synaptic plasticity/synapse models have been normally overlooked during the development of earlier supervised learning algorithms in SNNs [2], [4]–[13] as most of them use only the long-term plasticity models (constant weight) [20]–[22].

Based on the current research in neuroscience, biological synaptic plasticity models can be broadly classified into two categories, viz., homosynaptic plasticity or heterosynaptic plasticity. In homosynaptic plasticity models, the properties of the synapses are modified by their internal activities (activities of the neurons that are connected by the same synapses), and in heterosynaptic plasticity models, the properties of the synapses are modified by external activities (e.g., modulatory substances, such as acetylcholine, dopamine, histamine, and serotonin). Heterosynaptic plasticity models are beyond the scope of the work of this paper and are not highlighted here. The main focus here is only on the dynamic models of homosynaptic plasticity that are mainly used in SNNs, viz., that of short-term plasticity models [23]–[28]. Static

Manuscript received January 9, 2017; revised September 8, 2017, February 25, 2018, May 25, 2018, and July 28, 2018; accepted September 3, 2018. Date of publication September 26, 2018; date of current version March 18, 2019. *(Corresponding author: Suresh Sundaram.)*

The authors are with the School of Computer Science and Engineering, Nanyang Technological University, Singapore 639798 (e-mail: abeegith1@e.ntu.edu.sg; ssundaram@ntu.edu.sg; ensundara@ntu.edu.sg).

Color versions of one or more of the figures in this paper are available online at http://ieeexplore.ieee.org.

Digital Object Identifier 10.1109/TNNLS.2018.2868874

homosynaptic plasticity models will also not be discussed further here as it has been pointed out in [23] and [29] that an SNN with a dynamic plasticity has more computational power than that with only a static plasticity (long-term plasticity).

Short-term plasticity models include the release of neurotransmitters [23] in synaptic connections. Both facilitation [26] and depression [24], [25] can also be modeled in short-term plasticity models. These short-term plasticity models can be interpreted as neural connections with event-driven dynamic weights. However, the weights in this model recover to constant values in the absence of spiking activity and are the same as that of a long-term plasticity model with constant weights.

In a supervised learning framework, incorporating short-term plasticity models has been a challenging task. An SNN with a dynamic synapse model in [23] was developed for speech recognition task, and it has shown that a simple two-layer network can perform well for the selected data set. However, this system is failed when applied to a large database [30]. Further improvements to that network's architecture and algorithm to estimate the parameters of the dynamic synapses were proposed in [31] and [32]. Recently, an SNN for pattern classification called SWAT [3], which uses a dynamic synapse model [26] along with a long-term plasticity model, was presented. However, from the results presented for SWAT, it can be observed that the resulting network is large and involves a high computational load. Besides the challenges in implementing short-term plasticity, it is also important to note that the short-term plasticity models can only be employed on top of constant weights (long-term plasticity).

Instead of implementing the biological short-term plasticity models on top of long-term plasticity models, in this paper, we propose a new method to model a dynamic synapse suitable for SNNs by distributing the long-term plasticity over a specific time window (interval). With this objective, we present a time-varying synaptic efficacy function ($w_{ij}(t)$) as the weight instead of a constant synaptic weight (w_{ij}) to model a synapse. The synaptic efficacy function is defined as a summation of different amplitude-modulated Gaussian distribution functions with their centers located at different times in the time window. In this paper, using this newly defined Synaptic Efficacy Function-based leaky-integrate-and-fire neuRON model is referred to as SEFRON. This SEFRON model is then used for developing the learning algorithm for SNNs. This $w_{ij}(t)$ approximates the amplitude variation required in a weight within a time window based on both the presynaptic and postsynaptic activities for all the training patterns in that time window. Hence, the final weight of a single synaptic connection is a continuous time-varying function that is independent of incoming presynaptic spikes during the time window.

Recently, in the neuroscience literature, an interesting switching phenomenon has been observed in a synapse. This mechanism is such that it switches the same synapse from an excitatory nature to inhibitory nature, and vice versa [33], [34]. This switching phenomenon has been referred to as the gamma-aminobutyric acid (GABA)-switch. This phenomenon has been observed during the development of a human brain. In an infant's brain, GABA receptor-mediated responses are producing excitatory postsynaptic potentials. During the development of the adult brain (exclusively), it has been observed that the GABA receptor-mediated postsynaptic potential changes from excitatory to inhibitory nature [33]. In addition, experiments conducted on lactating rats have shown that the GABA receptor-mediated responses in oxytocin and vasopressin neurons are converted back into excitatory in a reversible manner [34]. These studies show that the GABA-switch occurs when there is a physiological need. Inspired by this phenomenon, in this paper, we have not restricted the proposed time-varying synaptic model ($w_{ij}(t)$) in SEFRON to be either excitatory or inhibitory nature, i.e., the weight is allowed to change in a continuous manner from a positive value to a negative value, and vice versa during the specified time window.

For pattern classification problems, using this SEFRON model, we also present a supervised learning algorithm to determine $w_{ij}(t)$ using a normalized form of the standard spike-timing-dependent plasticity (STDP) rule. For a given pattern, the supervised learning rule first calculates V_{STDP}, the postsynaptic potential due to the fractional contributions (or in other words normalized form of STDP). Then, it computes the change in the weight (amplitude of the $w_{ij}(t)$) by minimizing an error function based on the desired and actual postsynaptic spike times. This error function e is represented by the difference in the ratios of the firing threshold (θ) to the V_{STDP} of selected presynaptic spikes for the desired and actual postsynaptic spike times. Next, the learning rule uses the computed weight change to update $w_{ij}(t)$ by forming its product with a Gaussian distribution function centered at the selected presynaptic spike times. As a consequence of SEFRON's learning rule, $w_{ij}(t)$ for some synapses may have both positive and negative values within the time window, which imitates the GABA-switch phenomenon.

The computational power of a single SEFRON is then illustrated using a binary classification problem. Here, the class labels for both classes are coded into two different desired postsynaptic spike times ($\hat{t}_d^1, \hat{t}_d^2$). For classification purposes, the postsynaptic spike interval is split into two regions, such that each of the desired postsynaptic spike times falls within only one of the regions. The splitting time is defined as the boundary spike time ($\hat{t}_b$). Classification decision is made by the occurrence of the actual postsynaptic spike ($\hat{t}_a$) with respect to the boundary spike time, i.e., the class label is determined as class 1 if the postsynaptic spike occurs before the boundary spike time ($\hat{t}_a < \hat{t}_b$) and class 2 otherwise ($\hat{t}_a > \hat{t}_b$). Furthermore, a skipping sample strategy similar to that was used in [35] has been employed to prevent overtraining. A detailed performance evaluation of SEFRON is presented using four of the UCI machine learning data sets and its performance is compared with four well-known SNN algorithms, viz., SpikeProp [2], SWAT [3], online spiking neural network (OSNN) [9], and SRESN [7]. Based on the results, it can be seen that a single SEFRON outperforms all the other online learning SNN algorithms [7], [9]. The results also show that SEFRON produces similar accuracies as that of other off-line learning SNN algorithms [2], [3] but with a single SEFRON.

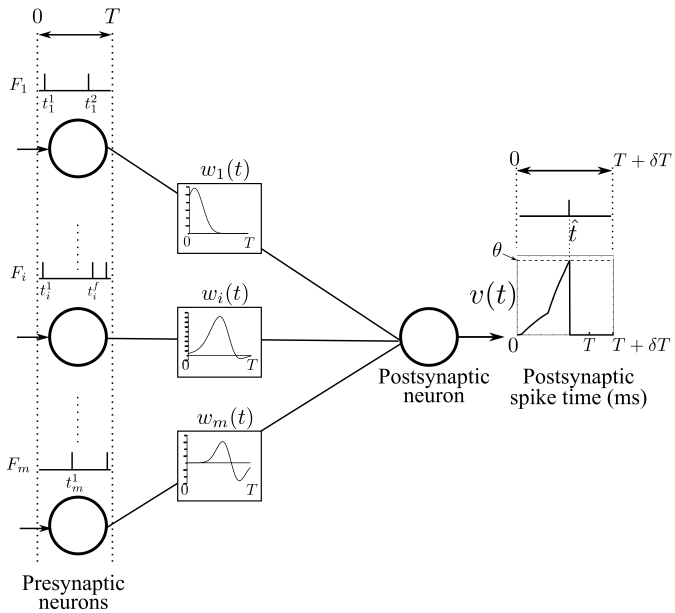

Fig. 1. SEFRON model with m number of synapses. Presynaptic spike time for a given input pattern is in the interval of $[0, T]$ ms, and postsynaptic spike time is in the interval of $[0, T + \delta T]$ ms.

The rest of this paper is organized as follows. The SEFRON model and its learning rule are highlighted in Section II. The functioning of a single SEFRON as a classifier is illustrated in Section III. The detailed performance comparison of SEFRON with other existing learning algorithms is presented in Section IV. Finally, the conclusions from this paper are summarized in Section V.

II. Development of SEFRON Model and Its Learning Rule

In this section, the details of the proposed SEFRON model along with its learning algorithm are described. Existing synapse models require different synapses to model both the excitatory and inhibitory characteristics, resulting in a larger network to encode the data distribution on a feature space. However, it is shown that the proposed synapse model is able to encapsulate the data distribution with a single neuron.

A. Single SEFRON Model

Fig. 1 shows a single LIF neuron with the time-varying long-term synapse model (SEFRON). A set of input synapses $\Gamma = \{1 \text{ to } m\}$ are connected to a postsynaptic neuron. The set of presynaptic spike times F_i of the ith synapse ($i \in \Gamma$) is defined as

$$F_i = \left\{t_i^k; 1 \leqslant k \leqslant n_i\right\} \tag{1}$$

where n_i is the total number of presynaptic spikes fired by the ith synapse and k represents the order of the firing. t_i^k is the firing time of the kth presynaptic spike fired by the ith input neuron. Let the presynaptic spike times for a given input pattern be in the time window (interval) $[0, T]$ ms. The postsynaptic firing time is represented by $\hat{t}$ and is set in the interval $[0, T + \delta T]$ ms with the limit of postsynaptic spike time extended by δT to capture the late postsynaptic spikes and also to allow the SEFRON model to fire a postsynaptic spike at a later time.

Since a single postsynaptic neuron model is used in this paper, the notation for the synaptic efficacy function between the ith input neuron and the output neuron is denoted as $w_{i1}(t)$, but for simplicity, it is written as $w_i(t)$. The postsynaptic potential $v(t)$ of SEFRON is defined as the summation of the product of the spike response of the presynaptic spike and the momentary weight determined by $w_i(t)$ for all presynaptic spikes (fired by all synapses). It is defined as

$$v(t) = \sum_{i=1}^{m} \sum_{k=1}^{n_i} w_i\left(t_i^k\right) \cdot \epsilon\left(t - t_i^k\right) \tag{2}$$

where $\epsilon(t)$ is the spike response function [2] and is given as

$$\epsilon(t) = \frac{t}{\tau} \exp\left(1 - \frac{t}{\tau}\right) \tag{3}$$

τ is the time constant of LIF neuron and $w_i(t_i^k)$ refers to the momentary synaptic efficacy (weight) and is the value of $w_i(t)$ at $t = t_i^k$

$$w_i\left(t_i^k\right) = \{w_i(t)|_{t=t_i^k}\}. \tag{4}$$

SEFRON fires a postsynaptic spike when the postsynaptic potential reaches firing threshold θ. The postsynaptic firing time $\hat{t}$ is defined as

$$\hat{t} = \{t | v(t) = \theta\} \tag{5}$$

where

$$\theta = v(\hat{t}) = \sum_{i=1}^{m} \sum_{k=1}^{n_i} w_i\left(t_i^k\right) \cdot \epsilon\left(\hat{t} - t_i^k\right). \tag{6}$$

As $w_i(t)$ is a time-varying function of synaptic efficacy with respect to presynaptic spike time, the interval for $w_i(t)$ is also set to $[0, T]$ ms to coincide with the interval of presynaptic spike times.

B. SEFRON's Learning Rule

The principles behind SEFRON's learning rule are briefly explained in the following. First, the learning rule computes $V_{\mathrm{STDP}}(\hat{t})$ using the fractional contribution of presynaptic spikes resulting in the "actual" postsynaptic spike time and also computes the same for the "desired" postsynaptic spike time. Next, it computes the change in the synaptic efficacy by minimizing an error function, which represents the difference in the ratio of θ to $V_{\mathrm{STDP}}(\hat{t})$ at the desired and actual postsynaptic spike times. Finally, the learning rule modulates the change in synaptic efficacy using a Gaussian distribution function centered at the current presynaptic spike time.

A normalized form of STDP-based rule is used [12] to compute the fractional contribution of presynaptic spikes for a given postsynaptic spike. The general STDP learning rule defines the synaptic efficacy change $\delta w(s)$ for a delay s between the presynaptic and postsynaptic firing time as

$$\delta w(s) = \begin{cases} +A_+ \cdot \exp(-s/\tau_+) & \text{if } s \geqslant 0 \\ -A_- \cdot \exp(s/\tau_-) & \text{if } s < 0 \end{cases} \tag{7}$$

where $(A_+,\ \tau_+)$ and $(A_-,\ \tau_-)$ are the maximum values of weight changes and plasticity window for the long-term potentiation and long-term depression, respectively. Since only one postsynaptic spike is used in SEFRON to determine the fractional contributions, the presynaptic spikes fired after the first postsynaptic spike are ignored. For example, in pattern classification problems, the first postsynaptic spike is important. Hence, other postsynaptic spikes are ignored. Therefore, A_- is assumed to be 0 in the SEFRON's learning rule. The fractional contribution $u_i^k(\hat{t})$ by a presynaptic spike t_i^k to fire a postsynaptic spike at $\hat{t}$ is the normalized STDP (as in [12]) and is calculated as

$$u_i^k(\hat{t}) = \frac{\delta w\left(\hat{t} - t_i^k\right)}{\sum_{i=1}^{m} \sum_{k=1}^{n_i} \delta w\left(\hat{t} - t_i^k\right)}. \tag{8}$$

The term $u_i^k(\hat{t})$ is independent of variable A_+ and depends only on the plasticity window τ_+. Note that the sum of all the fractional contributions $u_i^k(\hat{t})$ is equal to 1

$$\sum_{i=1}^{m} \sum_{k=1}^{n_i} u_i^k(\hat{t}) = 1. \tag{9}$$

Fractional contributions can also be used to measure the importance of presynaptic spikes to fire a postsynaptic spike at any specific time. A higher value for fractional contribution $u_i^k(\hat{t})$ indicates that the presynaptic spike at time t_i^k is more important than other presynaptic spikes for firing the postsynaptic spike at time $\hat{t}$. It can be noted that presynaptic spikes closer to a postsynaptic spike will have a higher fractional contribution value compared with presynaptic spikes that are further away from a postsynaptic spike.

The postsynaptic potential due to fractional contribution $V_{\mathrm{STDP}}(\hat{t})$ can be interpreted as the ideal postsynaptic potential at the time of firing if the STDP rule is employed in determining the weight. $V_{\mathrm{STDP}}(\hat{t})$ at time $\hat{t}$ is determined by replacing the momentary weight $w_i(t_i^k)$ with fractional contribution $u_i^k(\hat{t})$ in (6)

$$V_{\mathrm{STDP}}(\hat{t}) = \sum_{i=1}^{m} \sum_{k=1}^{n_i} u_i^k(\hat{t}) \cdot \epsilon\left(\hat{t} - t_i^k\right). \tag{10}$$

However, this $V_{\mathrm{STDP}}(\hat{t})$ may not be always equal to the firing threshold (θ) (except in the ideal case) due to variations in the input data. Therefore, the ratio of firing threshold θ to $V_{\mathrm{STDP}}(\hat{t})$ is used as the measure to determine the overall strength $(\gamma_{\hat{t}})$ required by all the synapses to make the firing possible at time $\hat{t}$ as in (10)

$$\theta = \gamma_{\hat{t}} \cdot V_{\mathrm{STDP}}(\hat{t}) = \gamma_{\hat{t}} \cdot \sum_{i=1}^{m} \sum_{k=1}^{n_i} u_i^k(\hat{t}) \cdot \epsilon\left(\hat{t} - t_i^k\right) \tag{11}$$

where the overall strength $\gamma_{\hat{t}}$ is calculated as

$$\gamma_{\hat{t}} = \frac{\theta}{V_{\mathrm{STDP}}(\hat{t})}. \tag{12}$$

In a supervised learning framework, a desired output is given and compared with the actual output. The weight is then adjusted to correct the differences between the desired output and the actual output. Here, the desired and actual outputs are the desired postsynaptic spike time $(\hat{t}_d)$ and the actual postsynaptic spike time $(\hat{t}_a)$, respectively. Instead of directly computing the differences in the postsynaptic spike times, we have defined an error function that can compute the differences in the overall strength due to the differences in desired and actual postsynaptic spike times

$$e = \gamma_{\hat{t}_d} - \gamma_{\hat{t}_a} = \frac{\theta}{V_{\mathrm{STDP}}(\hat{t}_d)} - \frac{\theta}{V_{\mathrm{STDP}}(\hat{t}_a)} \tag{13}$$

where $\gamma_{\hat{t}_d}$ and $\gamma_{\hat{t}_a}$ are the overall strengths due to the desired and actual postsynaptic spike times, respectively.

This error e can be directly used to determine the change in weight. It can be noted by comparing (6) and (11) that the ideal momentary weight is the product of overall strength and fractional contribution $[w_i(t_i^k) = \gamma_{\hat{t}}.u_i^k(\hat{t})$ for the ideal case]. Multiplication of the error e in the overall strength with the fractional contribution for the desired postsynaptic spike time ensures that the actual momentary weight moves in a direction toward the ideal momentary weight. This ensures that the actual postsynaptic spike time $(\hat{t}_a)$ moves toward the desired postsynaptic spike time $(\hat{t}_d)$. The individual change in the synaptic efficacy $\triangle w_i(t_i^k)$ for the ith synapse at a presynaptic spike time t_i^k is calculated by multiplying the error in overall strength with the fractional contribution for the desired postsynaptic spike time

$$\triangle w_i\left(t_i^k\right) = \lambda \cdot u_i^k(\hat{t}_d) \cdot e \tag{14}$$

where λ is the learning rate and usually set to a smaller value. Equation (14) can be expanded as

$$\triangle w_i\left(t_i^k\right) = \lambda \cdot \left(\gamma_{\hat{t}_d} \cdot u_i^k(\hat{t}_d) - \gamma_{\hat{t}_a} \cdot u_i^k(\hat{t}_d)\right) \tag{15}$$

where $\gamma_{\hat{t}_d} \cdot u_i^k(\hat{t}_d)$ is the ideal momentary weight. The other term $\gamma_{\hat{t}_a} \cdot u_i^k(\hat{t}_d)$ is calculated from the actual postsynaptic spike time for a given pattern, and it is not equal to the actual (current) momentary weight $w_i(t_i^k)$.

The change in synaptic efficacy computed here is a single value for a given input pattern. For other patterns that are similar to the current pattern, the synaptic efficacies should be similar. Hence, the current value of the synaptic efficacy is embedded in a time-varying function (a modulating function) that produces weights that are similar to the current one if the presynaptic spikes are nearer. In this paper, a Gaussian distribution function is chosen as the modulating function. $\Delta w_i(t_i^k)$ at single time instance t_i^k is embedded in a time-varying function $g_i^k(t)$ as

$$g_i^k(t) = \triangle w_i\left(t_i^k\right) \cdot \exp\left(\frac{-(t - t_i^k)^2}{2\sigma^2}\right) \tag{16}$$

where σ is the efficacy update range. A smaller value for σ would capture more variations in the synaptic efficacy, and an infinite value for σ would result in a constant $g_i^k(t)$ that resembles a long-term plasticity model.

Each synapse fires multiple presynaptic spikes. A time-varying synaptic efficacy function $w_i(t)$ for each synapse is obtained by adding all the changes in synaptic efficacy in an interval due to the different presynaptic spike times.

The synaptic efficacy function update rule for the ith synapse is

$$w_{i\text{new}}(t) = w_{i\text{old}}(t) + \sum_{k=1}^{n_i} g_i^k(t). \tag{17}$$

It can be noted that the updated $w_{i\text{new}}(t)$ may have both positive and negative values within the simulation interval. This imitates the GABA-switch phenomenon observed in a biological neuron.

III. SEFRON FOR PATTERN CLASSIFICATION PROBLEM

In this section, we illustrate the functioning of a single SEFRON for a binary pattern classification problem using a simple synthetic two-class linearly separable problem. In general, the input features of a pattern classification problem are real-valued and they have to be converted first into spike patterns. Here, the normalized input data x_i ($x_i \in [0, 1]$) is encoded into a spike pattern using the well-known population encoding scheme given in [2]. In the population encoding scheme, x_i is projected into multiple receptive field neurons to generate presynaptic spikes. Each receptive field neuron generates only one presynaptic spike. The total number of receptive field neurons (q) determines the total number of spikes that will be generated for a given input value. Each receptive field neuron h ($h \in [1, q]$) has a firing strength ϕ_i^h for the input data x_i, and it is computed as

$$\phi_i^h = \exp\left(-\frac{(x_i - \mu_h)^2}{2\sigma_{\text{pop}}^2}\right) \tag{18}$$

where μ_h and σ_{pop} are the center and the standard deviation of the hth receptive field neuron, respectively. μ_h and σ_{pop} are selected as in [2]

$$\mu_h = \frac{(2h-3)}{2 \cdot (q-2)} \tag{19}$$

$$\sigma_{\text{pop}} = \frac{1}{\beta \cdot (q-2)} \tag{20}$$

where β is the overlap constant [2].

The firing time of each presynaptic spike is

$$t_{i\_h}^1 = T \times \left[1 - \phi_i^h\right] \tag{21}$$

where T is the limit of the presynaptic spike time interval.

A. SEFRON Classifier

For a two-class problem, the class labels are coded into desired postsynaptic firing times as $\hat{t}_d^1$ for class 1 and $\hat{t}_d^2$ for class 2. Let $\hat{t}_b$ be the classification boundary referred to as the boundary spike time, and it should satisfy the condition, $\hat{t}_d^1 < \hat{t}_b < \hat{t}_d^2$. For classification, only the first actual postsynaptic spike $\hat{t}_a$ is used. Thus, any postsynaptic spikes fired after the first postsynaptic spike is ignored. If SEFRON does not fire any postsynaptic spike, the firing time of the postsynaptic spike is taken as the end of the simulation time.

1) Initialization: Here, the first training pattern is used to initialize $w_i(t)$ and θ. The ratio of threshold to postsynaptic potential due to the fractional contribution $[(\theta/V_{\text{STDP}}(\hat{t}_d))$ or $\gamma_{\hat{t}_d}]$ of the first sample is assumed to be 1. Hence, θ is set to the value of $V_{\text{STDP}}(\hat{t})_{\hat{t}=\hat{t}_d}$ using (10) and (11)

$$\theta := \sum_{i=1}^{m}\sum_{k=1}^{n_i} u_i^k(\hat{t}_d) \cdot \epsilon\left(\hat{t}_d - t_i^k\right). \tag{22}$$

If the actual postsynaptic firing time is the same as the desired firing time $\hat{t}_d$, then the following condition must be satisfied [see (6)]:

$$\theta = \sum_{i=1}^{m}\sum_{k=1}^{n_i} w_i\left(t_i^k\right) \cdot \epsilon\left(\hat{t}_d - t_i^k\right). \tag{23}$$

Hence, the initial momentary weight $w_i(t_i^k)$ of each synapse at the corresponding presynaptic spike time must be equal to $u_i^k(\hat{t}_d)$. The initial momentary weight is distributed using a Gaussian distribution function as

$$w_{i\text{initial}}(t) = \sum_{k=1}^{n_i} u_i^k(\hat{t}_d) \cdot \exp\left(\frac{-\left(t - t_i^k\right)^2}{2\sigma^2}\right). \tag{24}$$

In SEFRON, a sample is correctly classified if the postsynaptic spike is within the desired firing range (that is either fired after or before $\hat{t}_b$). The correctly classified samples are not used for updating $w_i(t)$. Avoiding the samples that do not add new knowledge during the training phase improves the generalization on the classwise data distribution [35]. For other samples, the SEFRON learning algorithm described in (8)–(17) is used.

B. Synthetic Binary Classification Problem

A linearly separable two-class synthetic classification problem is considered. It consists of two variables (x_1, x_2) belonging to two classes as given in the following:

$$\text{Class } 1 = \begin{cases} 0 \leqslant x_1 \leqslant 0.4 \\ 0 \leqslant x_2 \leqslant 0.4 \end{cases} \quad \text{Class } 2 = \begin{cases} 0.6 \leqslant x_1 \leqslant 1 \\ 0.6 \leqslant x_2 \leqslant 1. \end{cases}$$

100 random samples (50 from each class) are generated for building the training and testing sets. For the population encoding scheme, the total number of receptive field neurons q is set to 6 and the overlap constant β is set to 0.7 as in [7]. The total number of input presynaptic neurons in SEFRON is determined by the product of the number of receptive field neurons (q) and the dimension (m) of the input data. For this synthetic problem, the dimension of the input data m is 2. Hence, the total number of input neurons is 12. A bias presynaptic neuron is also added and set to fire at $t = 0$ s to ensure that the postsynaptic potential of all the inputs starts at $t = 0$ s.

The presynaptic spike interval limits T is set to 3 ms. Thus, the interval for $w(t)$ is also set to $[0, 3]$ ms to coincide with the spike interval. The postsynaptic spike interval is set to $[0, 4]$ ms (simulation time) to capture the late output spikes and also to model SEFRON to fire at a later time. The time constant of the spike response function has to be

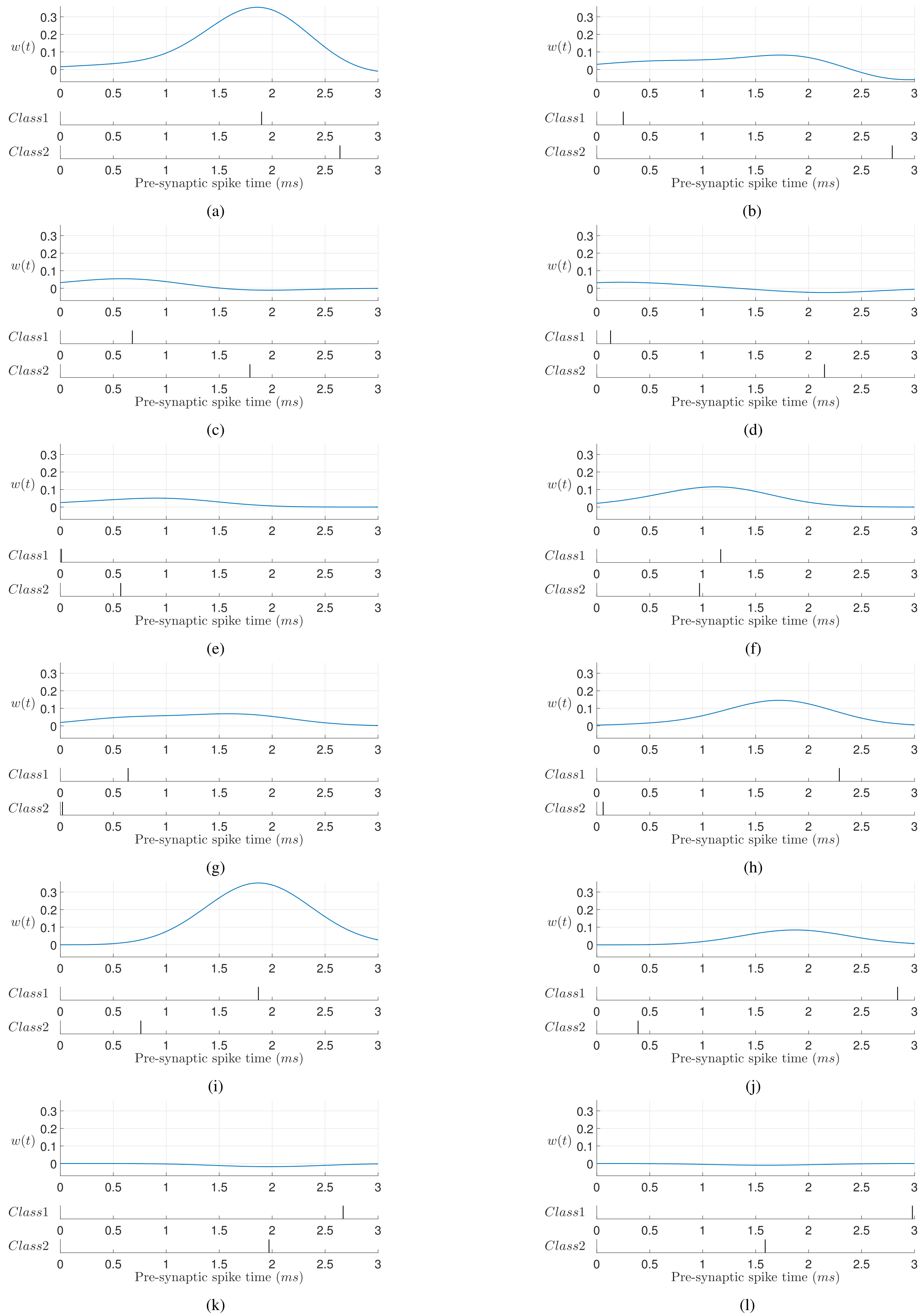

Fig. 2. $w(t)$ of all the input neurons and an example encoded input spike pattern for classes 1 and 2 sample. (a) Input neuron 1 of feature 1. (b) Input neuron 1 of feature 2. (c) Input neuron 2 of feature 1. (d) Input neuron 2 of feature 2. (e) Input neuron 3 of feature 1. (f) Input neuron 3 of feature 2. (g) Input neuron 4 of feature 1. (h) Input neuron 4 of feature 2. (i) Input neuron 5 of feature 1. (j) Input neuron 5 of feature 2. (k) Input neuron 6 of feature 1. (l) Input neuron 6 of feature 2.

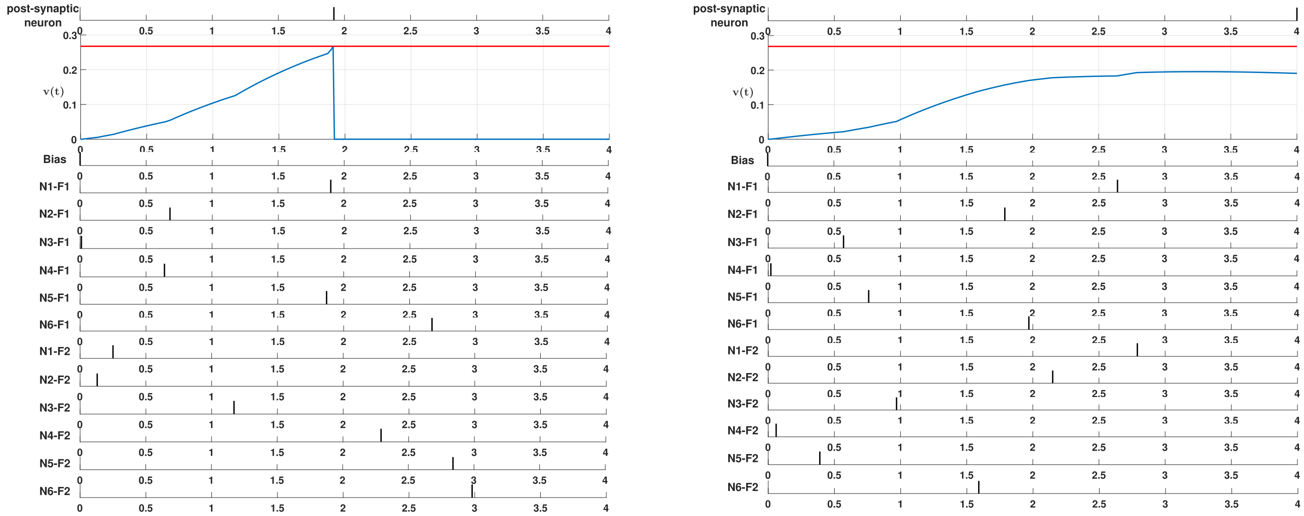

(a) (b)

Fig. 3. PSP of $c1$ and $c2$ for the encoded presynaptic spike time. Here, for example, N1-F1 refers to input neuron 1 of feature 1. (a) PSP of class 1 sample and its presynaptic spike time. (b) PSP of class 2 sample and its presynaptic spike time.

greater than the spike time interval for better convergence [2]. Hence, the time constant τ for a spike response function $\epsilon(t)$ is set to 3 ms. Desired spike firing times are the coded output labels for supervised learning. It has to be chosen within the simulation interval and also remain well separated. Hence, the desired firing time for $c1$ ($\hat{t}_d^1$) is set to the middle value of simulation time (2 ms), and for $c2$ ($\hat{t}_d^2$), it is set to the end value of simulation time (4 ms). These are the following four-algorithm-dependent parameters: the efficacy update range (σ), the plasticity window for STDP learning (τ_+), the learning rate (λ), and the boundary spike time ($\hat{t}_b$), and these are set as $\sigma = 0.5$ ms, $\tau_+ = 0.6$ ms, $\hat{t}_b = 3$ ms, and $\lambda = 0.5$, respectively.

For the performance evaluation, experiments were conducted in MATLAB R2015b using a 64-bit Windows 7 operating system in a CPU with 6 cores, 16-GB memory, and 3.2-GHz speed. SEFRON has achieved the performance of 100% classification accuracy for both the training and testing data sets. For this problem, functioning of SEFRON is described by selecting one training sample from class 1 $[x_1 = 0.3790, x_2 = 0.0217]$ and class 2 $[x_1 = 0.6041, x_2 = 0.6887]$. The encoded spike patterns for these real-valued $c1$ and $c2$ samples are [1.90, 0.68, 0.01, 0.64, 1.87, 2.67, 0.25, 0.13, 1.17, 2.29, 2.84, 2.98] and [2.64, 1.79, 0.57, 0.02, 0.76, 1.97, 2.79, 2.15, 0.97, 0.06, 0.39, 1.59] ms, respectively. These 12 encoded spike times are considered as the presynaptic firing times of the 12 input neurons. The times of the presynaptic spikes fired by all the input neurons for both classes and the final $w(t)$ obtained for all the 12 synapses at the end of the training are shown in Fig. 2.

In Fig. 2(a)–(d), the switching (in sign) similar to that of GABA-switch phenomenon can be observed in $w(t)$, indicating that those synapses can provoke both EPSP and IPSP for different presynaptic spike times. $w(t)$ in Fig. 2(e)–(j) are always positive, and therefore, they would only provoke an EPSP. On the other hand, in Fig. 2(k) and (l), $w(t)$ are always negative and would only provoke an IPSP. Due to the presence of the switching phenomenon in $w(t)$ in Fig. 2(b)–(d), the weights at the presynaptic spike times corresponding to $c1$ and $c2$ samples are positive and negative, respectively, thereby provoking an EPSP for $c1$ sample and IPSP for $c2$ sample.

The postsynaptic potential $v(t)$ for both input patterns along with the presynaptic/postsynaptic spikes is given in Fig. 3. For the $c1$ sample, the postsynaptic potential $v(t)$ crosses θ at 1.92 ms, resulting in a postsynaptic spike at the same time. however, the $c2$ sample $v(t)$ does not reach θ. Therefore, there is no postsynaptic spike, and hence, it is assumed to occur at the end of simulation interval. Due to the presence of the switching phenomenon in some synapses, it can be observed that the postsynaptic potential for the $c1$ input pattern is more positive when compared with the $c2$ input pattern.

C. Guidelines for Choosing the Parameter Values

The effects of the parameter setting on the performance of SEFRON were studied by changing one parameter at a time.

1) Effects of Efficacy Update Range (σ): Efficacy update range determines the effect of the weight change in the presynaptic spike time interval. A smaller value of σ captures more variation in the weight, and a larger value will result in minimal variation. Fig. 4 shows the effect of sigma on the accuracy. From Fig. 4, it can observed that the value for σ between 0.05 and 0.55 ms gives the best performance for SEFRON. It is also seen that for $\sigma \geqslant 1.5$ ms, the performance of SEFRON is nearly constant and very low. For this σ value, functioning of SEFRON is similar to that of an LIF neuron with a fixed weight. σ was set at 0.5 ms.

2) Effects of STDP Learning Window (τ_+): Fig. 5 shows the effect of τ_+ on the performance of SEFRON for the synthetic problem. The STDP learning window determines the contribution of each presynaptic spike for the change in weight. The contributions of the presynaptic spikes that fired

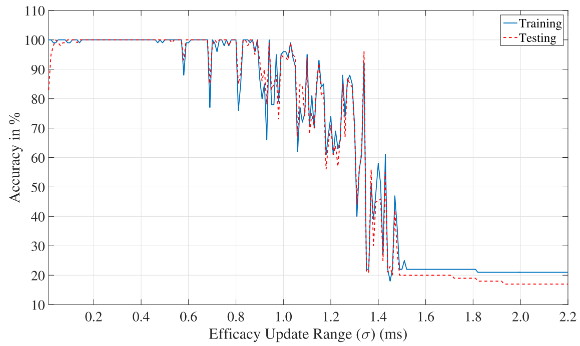

Fig. 4. Effects of σ on the performance of SEFRON.

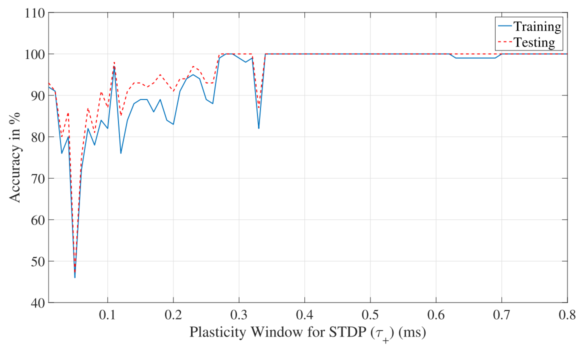

Fig. 5. Effects τ_+ on the performance of SEFRON.

much earlier to the postsynaptic spike increase and that fired closer to the postsynaptic spike decrease with increasing τ_+. From Fig. 5, it can be seen that $\tau_+ > 0.35$ ms gives the best performance. Here, τ_+ was set as 0.6 ms.

Based on these studies, the general guidelines for selecting the most dominant parameters of SEFRON learning rule σ and τ_+ can be given as follows: 0.05 ms $\leqslant \sigma \leqslant$ 0.55 ms and $\tau_+ > 0.35$ ms. Two other hyperparameters, namely, the boundary spike time $\hat{t}_b$ and the learning rate λ, are problem-dependent and are chosen appropriately using cross validation. Typically, choosing a middle value between the desired spike times for both classes $(\hat{t}_d^1, \hat{t}_d^2)$ is a good choice for $\hat{t}_b$. The learning rate is normally set at a smaller value lower than 1. A higher value may lead to oscillation in the weights.

IV. Performance Evaluation of SEFRON

The performance of the SEFRON classifier has been evaluated using four benchmark data sets from the UCI machine learning repository and compared with two off-line learning algorithms (SpikeProp [2] and SWAT [3]) and two online learning algorithms (SRESN [7] and OSNN [9]). Details of the training and testing sets, the number of features, and the number of classes used for the performance comparison are given in Table I. For each data set, 10 random trial sets were generated for both the training and testing data sets to perform a tenfold validation.

For each data set, based on the guidelines given in Section III-C, the values for the learning window, efficacy update range, boundary spike time, and learning rate were determined. Table II shows the selected values for these four parameters for each data set. The number of receptive field neurons in the population encoding scheme is set to 6, the same as given in [7] to maintain the consistency in the representation of the data sets. All the other LIF neuron parameters and computing platform are kept the same for all the studies and are given in Section III-B.

TABLE I
Description of Data Set Used for Validation

Dataset	# Features	# Classes	# Samples	
			Training	Testing
WBC	9	2	350	333
Ionosphere	33	2	175	176
PIMA	8	2	384	384
Liver	6	2	170	175

TABLE II
Parameter Values Chosen for Each Data Set

Data set	τ_+	σ	$\hat{t}_b$	λ
WBC	0.60	0.05	2.5	0.1
Ionosphere	0.55	0.15	3.0	0.5
PIMA	0.60	0.15	3.0	0.1
Liver	0.60	0.10	2.5	0.1

Results for all the other algorithms except for OSNN were generated using the same training and testing data sets, whereas the results for the OSNN have been reproduced from [9]. For SpikeProp, parameters were chosen following the guidelines given in [2] and 16 delayed terminals were used in the experimental study. Note that the number of neurons in the hidden layer is crucial in SpikeProp and it is determined by a constructive–destructive procedure as given in [36]. Since the population encoding scheme was used to generate the spike patterns, the parameter ISI in SWAT was set to 15–40 ms. The other parameters, viz., the frequency filter array, c_0 and A_p, were set to the same values as given in [3]. For SRESN, the same parameter settings given in [7] were used.

Based on the following four metrics, such as the architecture (size) of the network, the training accuracy, the testing accuracy, and the computation time, the performance of SEFRON has been compared with the other methods. The architecture of SNN is given in the form of $N_i : N_h : N_j$, where N_i, N_h, and N_j are the total number of inputs, hidden, and output neurons, respectively. The computation time was calculated as the average time taken to complete one epoch. Table III presents the performance comparison of SEFRON with other algorithms based on the four different data sets. The computation time for OSNN was not available, and hence, it is not reported in Table III.

From Table III, it can be seen that for the Wisconsin Breast Cancer (WBC) data set, the training and testing accuracies of all the methods are similar and also that they are higher compared with the accuracies of other data sets. Since the WBC is a linearly separable problem, the classification accuracy of SEFRON is on par with SpikeProp. SpikeProp achieves a similar classification accuracy with 15 hidden neurons and 2 neurons in the output layer, whereas SEFRON achieves the same with a single neuron.

TABLE III
PERFORMANCE COMPARISON

Dataset	Learning Algorithm	Architechture	Training Accuracy (%)	Testing Accuracy (%)	Avg training Epoch time (s)	Max No.of Epoch
WBC	SpikeProp	55:15:2	97.3(0.6)	**97.2(0.6)**	3.75	1000
	SWAT	54:702:2	96.5(0.5)	95.8(1.0)	265.85	500
	OSNN	54:(10-16):2	91.1(2.0)	90.4(1.8)	-	1
	SRESN	54:(5-8)	93.9(1.8)	94.0(2.6)	5.24	1
	SEFRON	**55:1**	**98.3(0.8)**	**96.4(0.7)**	**0.48**	100
Ionosphere	SpikeProp	199:25:2	89.0(7.9)	86.5(7.2)	6.37	3000
	SWAT	198:2574:2	86.5(6.7)	**90.0(2.3)**	462.18	500
	OSNN	198:(4-11):2	76.7(2.4)	76.6(4.8)	-	1
	SRESN	198:(6-13)	85.1(1.9)	79.3(3.0)	9.43	1
	SEFRON	**199:1**	**97.0(2.5)**	**88.9(1.7)**	**0.45**	100
PIMA	SpikeProp	49:20:2	78.6(2.5)	**76.2(1.8)**	3.83	3000
	SWAT	48:624:2	77.0(2.1)	72.1(1.8)	253	500
	OSNN	48:(8-18):2	68.2(2.0)	63.5(3.0)	-	1
	SRESN	48:(6-12)	67.0(0.8)	66.1(1.4)	5.08	1
	SEFRON	**49:1**	**84.1(1.5)**	**74.0(1.2)**	**0.39**	100
Liver	SpikeProp	37:15:2	71.5(5.2)	65.1(4.7)	2.65	3000
	SWAT	36:468:2	74.8(2.1)	60.9(3.2)	83.17	500
	OSNN	36:(4-7):2	58.7(2.2)	56.7(1.8)	-	1
	SRESN	36:(5-8)	59.8(1.2)	57.4(1.1)	1.74	1
	SEFRON	**37:1**	**91.5(5.4)**	**67.7(1.3)**	**0.15**	100

The Ionosphere data set is another data set that is easily separable. For this data set, the classification accuracy of SEFRON is closer to that of SWAT. On one hand, SWAT achieves a training accuracy of 86.5% and a testing accuracy of 90.0% with 2574 neurons in the hidden layer and 2 neurons in the output layer. On the other hand, SEFRON achieves 97.0% training accuracy and 88.9% testing accuracy with a single output neuron.

Based on the obtained results, it may be inferred that the Pima Indian diabetes (PIMA) data set and the Liver data set are not easily separable. Yet, the testing accuracy of SEFRON for the PIMA data set is closer to that of SpikeProp. However, SpikeProp requires 20 hidden layer neurons to learn the distribution with a 76.2% testing accuracy, whereas SEFRON achieves a 74.0% testing accuracy with only one output neuron. Similar observations can also be made for the Liver data set.

In summary, a single SEFRON classifier achieves a similar performance when compared with other methods that use larger networks. In addition, the computational time taken to train an SEFRON classifier is the lowest among all the other methods. The results clearly highlight that SEFRON is computationally more powerful compared with other LIF neuron-based networks with constant weights. Hence, replacing the constant weight with a time-varying weight reduces the size of the network and computational time while achieving similar performances.

V. CONCLUSION

In this paper, a new synapse model with a time-varying synaptic efficacy function incorporated in an LIF neuron, referred to as SEFRON, has been presented. A supervised learning rule for SEFRON is also proposed to approximate the functional relationship between the input and output spike patterns. Input–output correlation is encapsulated in the time-varying synaptic efficacy functions by adjusting the weights at different times. The SEFRON's learning rule computes the changes in weights (amplitude of the synaptic efficacy function) by minimizing an error function representing the difference in postsynaptic potential due to the fractional contributions of selected presynaptic spikes in a given pattern for both the desired and actual postsynaptic spikes. The resultant synaptic efficacy function can also change continuously from an excitatory to inhibitory nature, and this phenomenon is similar to the observed GABA-switch phenomenon in a biological neuron.

For binary classification problems, the performance of a single SEFRON has been compared with other well-known SNNs in the literature for four benchmark data sets from the UCI machine learning repository. The results indicate that a single SEFRON captures the classification decision boundary more efficiently and faster than other SNNs with multiple layer/neurons, thereby highlighting the high computational power of a spiking neuron with a time-varying synaptic efficacy function.

ACKNOWLEDGMENT

The authors would like to thank the reviewers for their comments that helped to improve the quality of this paper.

REFERENCES

[1] W. Maass, "Noisy spiking neurons with temporal coding have more computational power than sigmoidal neurons," Institue Theor. Comput. Sci., Graz Univ. Technol., Austria, Tech. Rep., 1999. [Online].Available:http://www.igi.tugraz.at/psfile

[2] S. M. Bohte, J. N. Kok, and H. L. Poutré, "Error-backpropagation in temporally encoded networks of spiking neurons," *Neurocomputing*, vol. 48, pp. 17–37, Oct. 2002.

[3] J. J. Wade, L. J. McDaid, J. A. Santos, and H. M. Sayers, "SWAT: A spiking neural network training algorithm for classification problems," *IEEE Trans. Neural Netw.*, vol. 21, no. 11, pp. 1817–1830, Nov. 2010.

[4] F. Ponulak and A. Kasiński, "Supervised learning in spiking neural networks with ReSuMe: Sequence learning, classification, and spike shifting," *Neural Comput.*, vol. 22, no. 2, pp. 467–510, 2010.

[5] R. Gütig and H. Sompolinsky, "The tempotron: A neuron that learns spike timing–based decisions," *Nature Neurosci.*, vol. 9, no. 3, pp. 420–428, 2006.

[6] A. Mohemmed, S. Schliebs, S. Matsuda, and N. Kasabov, "SPAN: Spike pattern association neuron for learning spatio-temporal spike patterns," *Int. J. Neural Syst.*, vol. 22, no. 4, p. 1250012, 2012.

[7] S. Dora, K. Subramanian, S. Suresh, and N. Sundararajan, "Development of a self-regulating evolving spiking neural network for classification problem," *Neurocomputing*, vol. 171, pp. 1216–1229, Jan. 2015.

[8] R. V. Florian, "The chronotron: A neuron that learns to fire temporally precise spike patterns," *PLoS ONE*, vol. 7, no. 8, p. e40233, 2012, doi: 10.1371/journal.pone.0040233.

[9] J. Wang, A. Belatreche, L. Maguire, and T. M. McGinnity, "An online supervised learning method for spiking neural networks with adaptive structure," *Neurocomputing*, vol. 144, pp. 526–536, Nov. 2014.

[10] S. Ghosh-Dastidar and H. Adeli, "A new supervised learning algorithm for multiple spiking neural networks with application in epilepsy and seizure detection," *Neural Netw.*, vol. 22, no. 10, pp. 1419–1431, 2009.

[11] O. Booij and H. tat Nguyen, "A gradient descent rule for spiking neurons emitting multiple spikes," *Inf. Process. Lett.*, vol. 95, no. 6, pp. 552–558, Sep. 2005.

[12] X. Xie, H. Qu, Z. Yi, and J. Kurths, "Efficient training of supervised spiking neural network via accurate synaptic-efficiency adjustment method," *IEEE Trans. Neural Netw. Learn. Syst.*, vol. 28, no. 6, pp. 1411–1424, Jun. 2017.

[13] J. Wang, A. Belatreche, L. P. Maguire, and T. M. McGinnity, "SpikeTemp: An enhanced rank-order-based learning approach for spiking neural networks with adaptive structure," *IEEE Trans. Neural Netw. Learn. Syst.*, vol. 28, no. 1, pp. 30–43, Jan. 2017.

[14] A. L. Hodgkin and A. F. Huxley, "A quantitative description of membrane current and its application to conduction and excitation in nerve," *J. Physiol.*, vol. 117, no. 4, pp. 500–544, 1952.

[15] R. B. Stein, "A theoretical analysis of neuronal variability," *Biophys. J.*, vol. 5, no. 2, pp. 173–194, 1965.

[16] R. B. Stein, "Some models of neuronal variability," *Biophys. J.*, vol. 7, no. 1, pp. 37–68, 1967.

[17] W. M. Kistler, W. Gerstner, and J. L. van Hemmen, "Reduction of the hodgkin-Huxley equations to a single-variable threshold model," *Neural Comput.*, vol. 9, no. 5, pp. 1015–1045, Jul. 1997.

[18] W. Gerstner, "Time structure of the activity in neural network models," *Phys. Rev. E, Stat. Phys. Plasmas Fluids Relat. Interdiscip. Top.*, vol. 51, pp. 738–758, Jan. 1995.

[19] W. Gerstner and W. M. Kistler, *Spiking Neuron Models: Single Neurons, Populations, Plasticity*. Cambridge, U.K.: Cambridge Univ. Press, 2002.

[20] D. O. Hebb, *The Organization of Behavior: A Neuropsychological Theory*, vol. 63. New York, NY, USA: Wiley, 1949.

[21] H. Markram, W. Gerstner, and P. J. Sjöström, *Spike-Timing-Dependent Plasticity: A Comprehensive Overview*. Lausanne, Switzerland: Frontiers Media, 2012.

[22] T. V. Bliss and T. Lømo, "Long-lasting potentiation of synaptic transmission in the dentate area of the anaesthetized rabbit following stimulation of the perforant path," *J. Physiol.*, vol. 232, no. 2, pp. 331–356, 1973.

[23] J.-S. Liaw and T. W. Berger, "Dynamic synapse: A new concept of neural representation and computation," *Hippocampus*, vol. 6, no. 6, pp. 591–600, 1996.

[24] M. V. Tsodyks and H. Markram, "Plasticity of neocortical synapses enables transitions between rate and temporal coding," in *Proc. ICANN*, 1996, pp. 445–450.

[25] M. V. Tsodyks and H. Markram, "The neural code between neocortical pyramidal neurons depends on neurotransmitter release probability," *Proc. Nat. Acad. Sci. USA*, vol. 94, no. 2, pp. 719–723, 1997.

[26] M. Tsodyks, K. Pawelzik, and H. Markram, "Neural networks with dynamic synapses," *Neural Comput.*, vol. 10, no. 4, pp. 821–835, 1998.

[27] L. F. Abbott, J. A. Varela, K. Sen, and S. B. Nelson, "Synaptic depression and cortical gain control," *Science*, vol. 275, no. 5297, pp. 221–224, 1997.

[28] J. S. Dittman, A. C. Kreitzer, and W. G. Regehr, "Interplay between facilitation, depression, and residual calcium at three presynaptic terminals," *J. Neurosci.*, vol. 20, no. 4, pp. 1374–1385, 2000.

[29] W. Maass and A. M. Zador, "Dynamic stochastic synapses as computational units," *Neural Comput.*, vol. 11, no. 4, pp. 903–917, 1999.

[30] A. A. Dibazar, H. H. Narnarvar, and T. W. Berger, "A new approach for isolated word recognition using dynamic synapse neural networks," in *Proc. Int. Joint Conf. Neural Netw.*, vol. 4, Jul. 2003, pp. 3146–3150.

[31] J.-S. Liaw and T. W. Berger, "Robust speech recognition with dynamic synapses," in *Proc. IEEE Int. Joint Conf. Neural Netw. World Congr. Comput. Intell.*, vol. 3, May 1998, pp. 2175–2179.

[32] H. H. Namarvar, J.-S. Liaw, and T. W. Berger, "A new dynamic synapse neural network for speech recognition," in *Proc. Int. Joint Conf. Neural Netw. (IJCNN)*, vol. 4, Jul. 2001, pp. 2985–2990.

[33] K. Ganguly, A. F. Schinder, S. T. Wong, and M. M. Poo, "GABA itself promotes the developmental switch of neuronal GABAergic responses from excitation to inhibition," *Cell*, vol. 105, no. 4, pp. 521–532, 2001.

[34] S. W. Lee *et al.*, "GABAergic inhibition is weakened or converted into excitation in the oxytocin and vasopressin neurons of the lactating rat," *Mol. Brain*, vol. 8, no. 1, p. 34, 2015.

[35] S. Suresh, K. Dong, and H. J. Kim, "A sequential learning algorithm for self-adaptive resource allocation network classifier," *Neurocomputing*, vol. 73, nos. 16–18, pp. 3012–3019, 2010.

[36] S. Suresh, S. N. Omkar, V. Mani, and T. N. G. Prakash, "Lift coefficient prediction at high angle of attack using recurrent neural network," *Aerosp. Sci. Technol.*, vol. 7, no. 8, pp. 595–602, 2003.

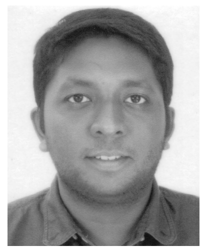

Abeegithan Jeyasothy received the B.Eng. degree in electrical and electronic engineering from Nanyang Technological University, Singapore, where he is currently pursuing the Ph.D. degree with the School of Computer Science and Engineering.

His current research interests include spiking neural networks and machine learning.

Suresh Sundaram (SM'08) received the B.E. degree in electrical and electronics engineering from Bharathiyar University, Coimbatore, India, in 1999, and the M.E. and Ph.D. degrees in aerospace engineering from the Indian Institute of Science, Bengaluru, India, in 2001 and 2005, respectively.

From 2005 to 2007, he was a Post-Doctoral Researcher with the School of Electrical Engineering, Nanyang Technological University, Singapore. From 2007 to 2008, he was a Research Fellow with the European Research Consortium for Informatics and Mathematics, National Institute for Research in Computer Science and Control, Nice, France. He was a Visiting Faculty Member in industrial engineering with Korea University, Seoul, South Korea, for a short period. In 2009, he was an Assistant Professor with the Department of Electrical Engineering, IIT Delhi, New Delhi, India. Since 2010, he has been an Associate Professor with the School of Computer Science and Engineering, Nanyang Technological University. His current research interests include flight control, unmanned aerial vehicle design, machine learning, and optimization and computer vision.

Narasimhan Sundararajan (LF'11) received the B.E. degree (Hons.) in electrical engineering from the University of Madras, Chennai, India, in 1966, the M.Tech. degree from IIT Madras, Chennai, in 1968, and the Ph.D. degree in electrical engineering from the University of Illinois at Urbana–Champaign, Urbana, IL, USA, in 1971.

From 1971 to 1991, he was with the Vikram Sarabhai Space Centre, Indian Space Research Organization, Trivandrum, India, where he was involved in different capacities. From 1991, he was a Professor with the School of Electrical and Electronic Engineering, Nanyang Technological University (NTU), Singapore, and retired from that position in 2010. He was a National Research Council Research Associate with the NASA's Ames Research Center, Ames, CA, USA, in 1974, and a Senior NRC Research Associate with the NASA's Langley Research Center, Hampton, VA, USA, from 1981 to 1986. He is currently a Senior Research Fellow with the School of Computer Engineering, NTU, where he is involved in air traffic management (ATM) research problems. He has published over 250 papers and written six books in the field of computational intelligence and neural networks. His current research interests include ATM, spiking neural networks, neuro-fuzzy systems, and optimization with swarm intelligence.